Nano-aperture array based optical imaging system on a microfluidic chip

Xin Heng[1], Xiquan Cui[1], Kevin W. Reynolds[2], David Erickson[3], Demetri Psaltis[1], Changhuei Yang[1]
[1]Department of Electrical Engineering, California Institute of Technology, Pasadena, CA, 91125; [2] Department of Physics, Norfolk State University, Norfolk, VA, 23504; [3] Mechanical and Aerospace Engineering, Cornell University, Ithaca, NY, 14853.
E-mail address: xin@caltech.edu

Abstract: We report the implementation of a novel nano-aperture array based imaging technique in a microfluidic network, termed "Optofluidic Microscopy (OFM)". The OFM prototype features high resolution, compact volume and capable of high-throughput sample imaging.

OCIS codes: (170.0170) Medical optics and biotechnology

In recent years, there has been a rapid development of microfluidic devices with numerous applications within the life sciences and clinical fields [1, 2]. The major advantages of these devices are their inherent compactness and low cost. However, one particular on-chip instrumentation need has not been satisfactorily addressed – high-resolution (sub-micron) on-chip optical imaging. High resolution imaging requirement in existing microfluidic systems is fulfilled by using bulky conventional microscopes [3, 4], obviating the cost and size advantages of micro analysis systems. In this paper, we demonstrate a novel imaging technique, termed Optofluidic Microscopy (OFM), which enables high-resolution and high-throughput imaging.

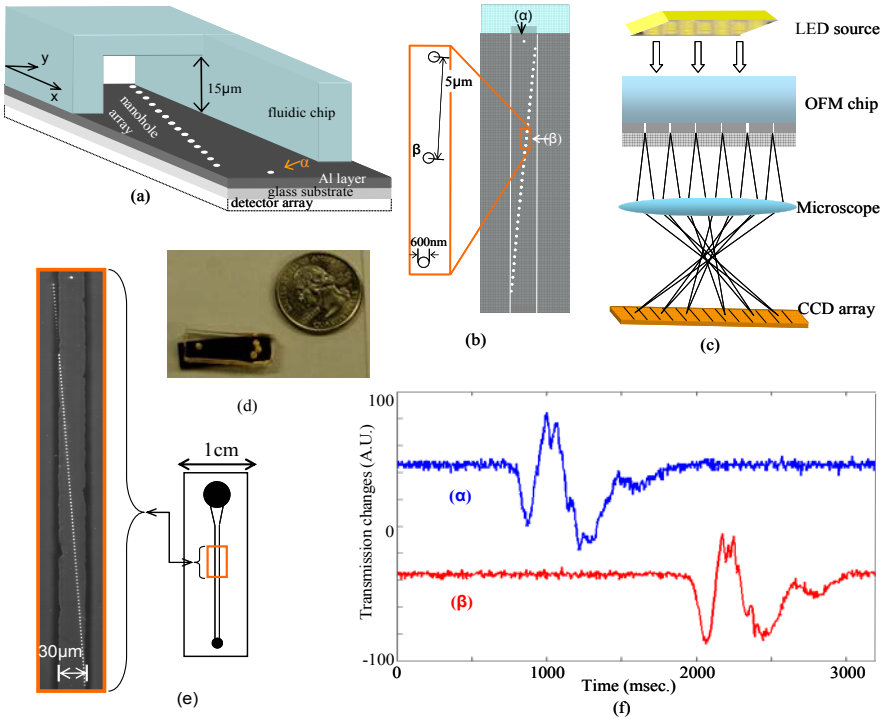

Figure 1 (a) Architecture of the Optofluidic Microscope (OFM); α denotes the isolated hole; (b) The top view of the OFM; β denotes the corresponding hole that scans the same line on the target as hole α does; (c) Experimental setup of the current OFM prototype; (d) Photograph of the OFM prototype compared with a U.S. quarter; the actual dimension of the OFM's active area is about the area of Mr. Washington's lips on the quarter; (e) Photograph of the orientation of the nanohole array with respect to the channel; channel width is about 30μm; (f) Transmission time traces from hole α (blue) and hole β (red).

The OFM device consists of a PDMS microfluidic chip bonded to a metal substrate with an etched array of nanoholes oriented at a small angle relative to the micro-channel (Fig. 1(a, b). The diameter of the nanoholes is 600 nm, and the metallic layer consists of an 80nm thick aluminum film. The nano-aperture array on the aluminum foil was defined by e-beam lithography and reactive ion etching. The microfluidic chip was produced by replica molding. The alignment of the fluidic layer and the metallic layer was accomplished by using a Suss mask aligner. A white LED light (Lamina BL3000) at normal incidence to the device provides the illumination (~0.1 W/cm^2). The spacing of the holes along the channel (denoted as x-direction) is 5μm. Fabrication of the prototype directly onto a sensor array is technically straightforward and thus here we concentrate on demonstrating the proof of principal and characterizing the optical system. In our present demonstration, the transmissions were relayed via a conventional microscope onto a CCD array as shown in Fig. 1(c).

1-55752-813-6/06/$25.00 ©2006 IEEE

The imaging of a target with an OFM device is accomplished by flowing it across the nanohole array. As it passes over, each individual nanohole will take a line scan of the target.

As the target flows over each hole at a different time, the compilation of the line scans will form a distorted transmission image, but this distortion can be corrected by taking an additional measurement of the flow velocity of the target (v). In our implementation, this parameter is determined by using an isolated nanohole at one end of the array (Fig. 1(a, b, e). By monitoring the time delay between the line scans through the isolated nanohole α and the corresponding hole β in the array, we can then determine v. This line scan pair serves a target rotation/ tumble monitor which enables us to screen out tumbling targets. Figure 1(f) shows a pair of line scans acquired by these two holes during the passage of an un-rotated target.

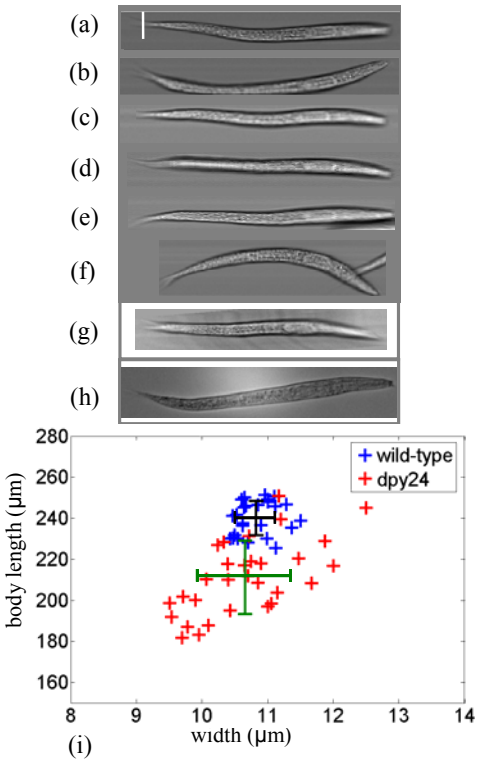

Figure 2 (a)-(f) Some OFM images of wild-type *C. elegans* larvae at the first larval stage; (g) OFM image of a dpy-24 mutant; note that the white bar represents 25μm for Fig.(a-g); (h) Conventional microscope image of a wild-type larva (not in the same scale as Fig.(a-g)); (i) Aspect ratio map of wild-type larvae (25 entities); aspect ratio map of dpy-24 mutants (31 entities). The black and green error bars represent the variation span of wild-type and mutant, respectively.

To evaluate the utility of the OFM systems for bioscience applications, we focus on one particular application – high-throughput *Caenorhabditis elegans* (*C. elegans*) imaging and population phenotyping. In many cases, body size and shape are two major phenotypes. However, the parameters that are characterized in current *C. elegans* research are mostly qualitatively described. To demonstrate the capability of our OFM for imaging *C. elegans*, we used a collection of wild-type *C. elegans* at the first larval stage. The sample was prepared by first euthanizing *C. elegans* in a 70°C heat bath for 3 minutes, and then mixing them with 0.1% BSA solution. Within the microfluidic channel, pressure driven flow was used to drive the targets. Fig. 2(a-f) shows some OFM images of the wild-type *C. elegans*, and Figure 2(h) shows the conventional microscope image of a *C. elegans*. It can be clearly seen that the OFM is capable of imaging the body profile of the *C. elegans*, as well as internal structures within the organisms.

To demonstrate the capability of the OFM system in nematode phenotyping, we acquired images from two separate populations of *C. elegans*: wild-type, and a dpy-24 mutant. Manual measurements of body length and width were taken from the acquired images. The data is plotted in Fig. 2(i). Average length of wild-type larva is 240.1 ± 8.3μm and its width is 10.8 ± 0.3μm; this renders a body aspect-ratio of 22.19 ± 0.88. Meanwhile, the length of dpy24 larva is 211.2 ± 17.9μm and its width is 10.7 ± 0.7μm; this gives an aspect ratio of 19.84 ± 1.35. The aspect-ratio map demonstrates a successful separation of these two genotypes, even if their difference in body shape at this early development stage is barely distinguishable by human eyes (see Fig. 2(a-g)).

In addition to *C. elegans* imaging, the OFM can also be used to image any micro-organisms or biological cells that can be suspended in a liquid medium. The simplicity and compact nature of OFM systems, and the fact that they can be created with existing fabrication technology should translate to their swift adaptation as important lab-on-a-chip components.

References:

[1] A. Y. Fu, C. Spence, A. Scherer, F. H. Arnold, and S. R. Quake, "A microfabricated fluorescence-activated cell sorter," *Nature Biotechnology*, vol. 17, pp. 1109-1111, 1999.

[2] J. O. Tegenfeldt, O. Bakajin, C. F. Chou, S. S. Chan, R. Austin, W. Fann, L. Liou, E. Chan, T. Duke, and E. C. Cox, "Near-field scanner for moving molecules," *Physical review letters*, vol. 86, pp. 1378-1381, 2001.

[3] D. Akin, H. B. Li, and R. Bashir, "Real-time virus trapping and fluorescent imaging in microfluidic devices," *Nano Letters*, vol. 4, pp. 257-259, 2004.

[4] J. B. Salmon, A. Ajdari, P. Tabeling, L. Servant, D. Talaga, M. Joanicot, and "In situ Raman imaging of interdiffusion in a microchannel," *Applied physics letters*, vol. 86, 2005.